Institute of Particle Physics (Canada) Summer Student Fellowship

Simon Fraser University, Burnaby, BC, Canada

Understanding Optical Noise for P-ONE: Analysis of ^{40}K (PRELIMINARY)

Student:

Matthew Ens

Supervisor:

Dr. Matthias Danninger (SFU)

August 14, 2020

Contents

1 Introduction **1**

1.1 The Pacific Ocean Neutrino Explorer (P-ONE) . . . 1

1.2 Pathfinder/Frontrunner: STRAW . . . 1

1.3 Project Overview . . . 4

2 Project Details **4**

2.1 Analysis of STRAW Data . . . 4

2.1.1 Looking for Coincidences . . . 6

2.2 Simulation of STRAW detector . . . 8

2.2.1 GEANT4 Simulation Details . . . 8

2.2.2 Detector Definition . . . 9

2.2.3 Quantum Efficiency . . . 11

2.2.4 Other Considerations . . . 11

2.2.5 Simulated Coincidences and Effective Volume . . . 13

2.3 Salinity Calculation from ^{40}K coincidences . . . 14

3 Future Work **15**

3.1 Other Sources of Noise . . . 15

3.1.1 Scintillation . . . 15

3.1.2 Bioluminescence . . . 15

3.2 Analysis of sDOM efficiency . . . 15

4 Conclusion **16**

5 Acknowledgements **16**

List of Figures

1 Planned P-ONE Telescope . . . 2

2 Diagram of POCAM and sDOM . . . 2

3 Diagram of STRAW detector . . . 3

4 Diagram of Time over Threshold . . . 5

5 Plots of a data file . . . 5

6 Coincident hits from Antares . . . 6

7 Example of a low noise . . . 7

8 Coincidences in STRAW data . . . 7

9 Plot of the simulated absorption lengths as a function of photon energy . . . 9

10 Comparison of simulated sDOM to actual sDOM . . . 10

11 Comparison of angular acceptances of simulated sDOM and actual sDOM . . . 10

12 Plot of PMT quantum efficiency . . . 11

13 Plot of simulated noise compared to STRAW data . . . 12

14 Coincidences in Simulation . . . 13

15 Plot of effective volume vs. radius . . . 14

Abstract

Progress was made towards a noise model for the P-ONE neutrino telescope using the STRAW detector with the main focus being modelling noise from Potassium-40.

A study of the noise from Potassium-40 (^{40}K) causing coincident hits on the detector was conducted and the salinity of the Cascaia Basin was found to be 12526 ± 752 ^{40}K decays per second per cubic metre which agreed with Ocean Netoworks Canada's measurement of the salinity within error. A simulation of STRAW was also created to model the noise from ^{40}K .

1 Introduction

1.1 The Pacific Ocean Neutrino Explorer (P-ONE)

The Pacific Ocean Neutrino Explorer (P-ONE) is a planned neutrino telescope set to be built in the Cascadia Basin, 2660m below sea level, off the coast of Vancouver Island. The Cascadia Basin is an ideal site for a neutrino telescope as a telescope here will allow us to observe new areas of the sky and Ocean Networks Canada (ONC) already has infrastructure to this site as part of their NEPTUNE ocean observatory.

Similar to other water or ice medium neutrino telescopes, P-ONE relies on the detection of Cerenkov photons from neutrinos passing through the ocean water in the vicinity of the telescope. The first stage of P-ONE is set to be deployed in 2023/2024 with an array of ten detector strings, see figure 1. Each string will consist of a number of optical modules (OMs) with photomultiplier tubes to detect the Cerenkov radiation from neutrinos incident on the detector. This array will have a cubic-kilometre scale volume with the ability for the telescope to be scaled up with further arrays.

1.2 Pathfinder/Frontrunner: STRAW

In order to characterize the Cascadia Basin site, the P-ONE collaboration has deployed STRAW (STRings for the Absorption length in Water). The STRAW detector consists of two strings, each with a combination of two instruments: the straw POCAM and sDOM, see Figure 3.[2]

The STRAW Precision Optical Calibration Module (POCAM) is a light-emitting calibration device for STRAW. With LEDs of different wavelengths, the STRAW POCAM can emit adjustable, isotropic light flashes with known intensity over nanosecond timescales. [2]

The sDOM is the light sensor for STRAW, it consists of two light detecting photomultiplier tubes situated inside glass hemispheres at opposite ends of a 60cm long cylinder which holds the electronics for the sDOM. See Figure 2

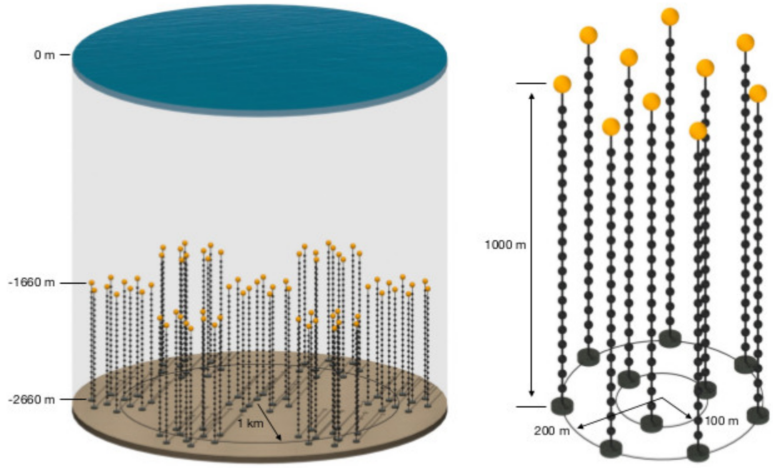

Figure 1: Left: The full-scale P-ONE telescope with several smaller arrays. Right: The 10 strings for stand-alone P-ONE, planned to be deployed in 2023/24. Taken from [1]

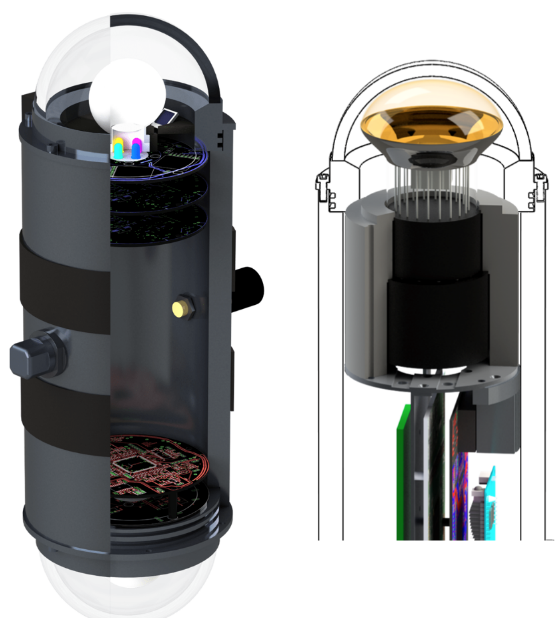

Figure 2: The STRAW modules. **Left:** The POCAM, used for emitting isotropic, adjustable flashes of different wavelengths. **Right:** One half of an sDOM, with the PMT and electronics inside. The other half of the sDOM is a mirror image of this. Figures taken from [2]

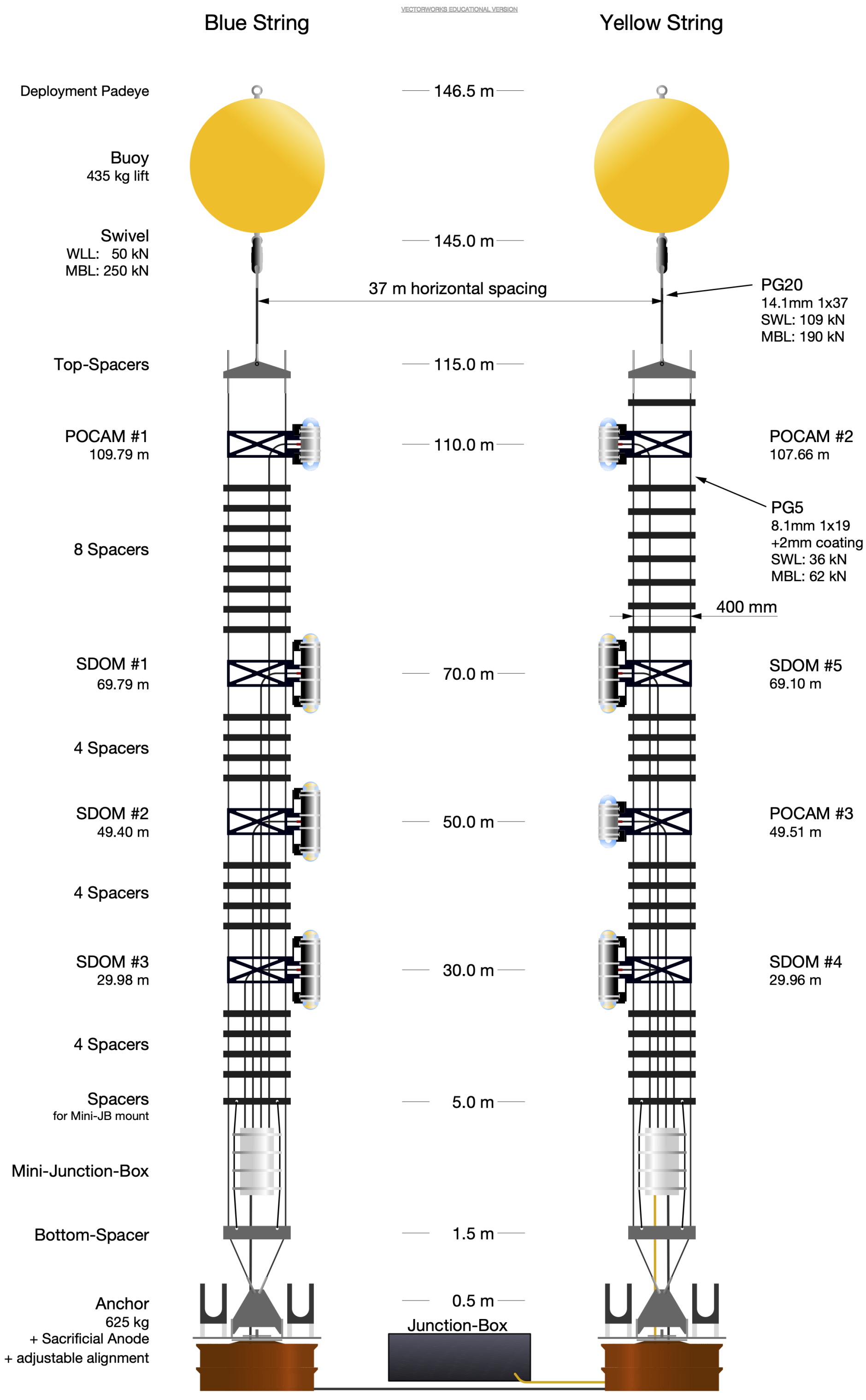

Figure 3: Diagram of STRAW detector. Two strings equipped with three POCAMs and five sDOMs. Taken from [1]

1.3 Project Overview

The deep ocean is usually imagined as dark and unchanging, an ideal place for the detection of the Cerenkov photons from passing neutrinos. When we take a closer look, however, we see that the Abyss is not as dark as it seems. Cerenkov light from the beta decay of Potassium-40 (^{40}K) dissolved in the ocean water along with bioluminescent organisms and scintillation in the glass of our detectors add to the challenge of detecting neutrinos and these sources of noise must be understood in order to design proper triggers for neutrino detection.

The main focus of my project for the summer was starting work on a noise model for P-ONE using the data from STRAW and GEANT4 [3] simulations of the sDOM. We decided to focus on noise from ^{40}K since the process of ^{40}K decay is well understood, making it more straightforward to model. The Cerenkov light that ^{40}K produces when it decays is also similar to the light produced by incoming neutrinos, making it the most important component of noise to understand.

2 Project Details

The work completed this summer can be split into two main components, analysis of the STRAW data and simulation of STRAW with GEANT4. Understanding how to work with and interpret the data is key to building an accurate noise model since we can compare the data to our own simulations to check our understanding of what is actually happening, while modelling the data in a simulation allows us to see what kind of noise there is, if any, and how to filter it out for actual physics events.

2.1 Analysis of STRAW Data

The sDOM uses a time-over-threshold data collection scheme with four channels for each photomultiplier tube (PMT). Each channel corresponds to a different number of detected photoelectrons, see Figure 4. Since each sDOM contains two PMTs, a STRAW data file will list the channel of a detection (1-4 for upward PMT, 5-8 for downward PMT, and 0,9 for timing), whether the time listed is a rising or falling edge (see figure 4), and the time the detection occurred at in nanoseconds. See appendix for a sample STRAW data file.

Using Python and Numpy as our analysis code, plots can be made of the detection rate over a data run (usually 60s) or of the time differences between consecutive hits for a particular sDOM and channel. See Figure 5. Other analyses can be done as well.

One analysis we found interesting was done by another neutrino telescope, ANTARES [4]. In their study, they measured the time differences between photons that struck different PMTs at roughly (within 25ns) the same time

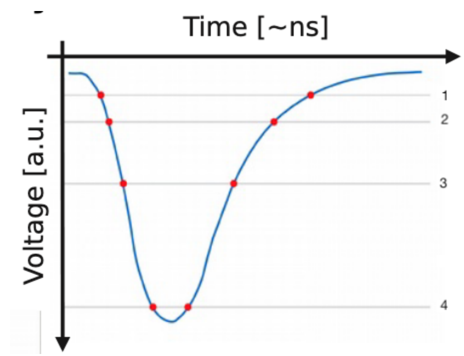

Figure 4: A voltage plot for a PMT with the thresholds drawn in. Times will be recorded when the voltage crosses each threshold, a 'rising' edge corresponding to crossing from a lower threshold to a higher threshold and a 'falling' edge corresponding to crossing from a higher threshold to a lower threshold.

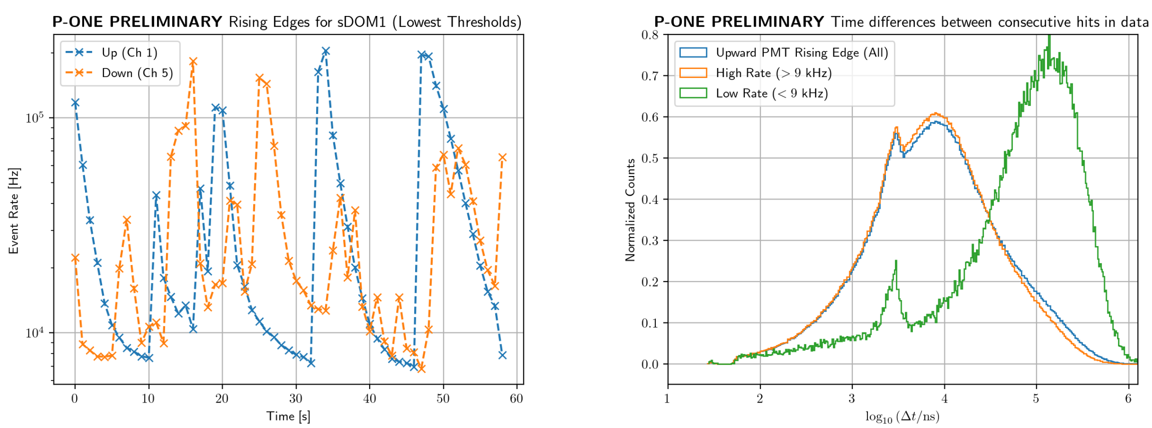

Figure 5: Plots of a data sample. **Left:** A plot of the detection rate over one minute of data for the lowest thresholds on both the upward and downward facing PMTs of sDOM 1. **Right:** A plot of the time differences between consecutive hits for the lowest threshold of the upward facing PMT. The blue curve is split into 'high' (orange) and 'low' (green) noise times based on whether each particular second fell above or below the arbitrary low noise threshold of 9 kHz. Note the x-axis is plotted on a log scale. Results are **PRELIMINARY**

and were able to correlate the distribution of these "coincident" hits with the decay rate of ^{40}K in the water and find the salinity of the ocean water from this activity.[4] Since the salinity of the ocean stays approximately constant they could track the salinity measured by their detectors over time and use these measurements to monitor the efficiency of their detectors.[4] We performed this analysis with the STRAW data using coincident detections from the upward and downward facing PMTs of each sDOM. With this analysis we hoped to be able to calculate the salinity of the Cascadia Basin from ^{40}K and compare this result to salinity measurements of the Cascadia Basin from Ocean Networks Canada (ONC). This analysis would be the first measurement with the STRAW detector aside from detecting flashes from the POCAMs and would allow us to get a full understanding of our detector and the nature of ^{40}K noise in the Cascadia Basin.

2.1.1 Looking for Coincidences

The study [4] focused on looking for coincident detections on multiple PMTs. A coincident detection is found when two PMTs record a detection within 25ns of each other. Since we have no way of knowing where a detected photon originated from, each coincidence could be “genuine”, where the photons detected by both PMTs came from the same event (^{40}K decay) or “false”, where two photons happened to be recorded at approximately the same time but are not from the same event. Since false false coincidences occur randomly they should happen evenly over the entire 50ns whereas genuine coincidences will be more prevalent near $\Delta t = 0$ which will produce a curve that is normally distributed with a mean close to 0. A plot of these coincidences from the ANTARES study can be seen in Figure 6.

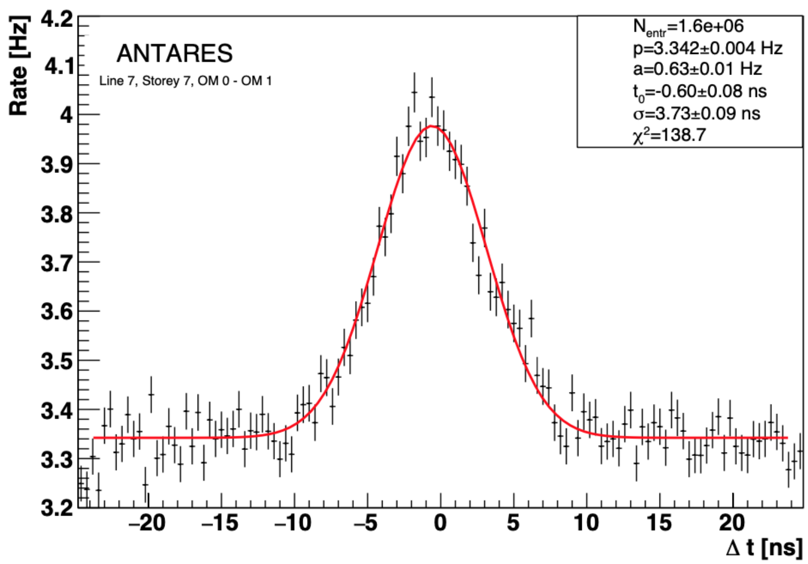

Figure 6: Detected hit time differences, Δt, from two adjacent DOMs in ANTARES detector with Gaussian fit parameters listed. Taken from [4]

Each sDOM only has two PMTs (upward facing and downward facing) so we looked for coincident detections between these two. Since the noise rate from ^{40}K is low compared to other sources of noise such as bioluminescence we decided to focus on searching the lowest threshold of the data for these coincidences. This still proved to be too full of false coincidences for any distribution of genuine coincidences to emerge so we narrowed our search to sections of data with a detection rate of less than 20 kHz (20 hits per ms). An example of such a time can be seen in Figure 7.

By searching for coincidences only in these ultra-low noise times, we were able to extract enough genuine coincidences from the data to produce a similar distribution to the ANTARES study, as seen in Figure 8.

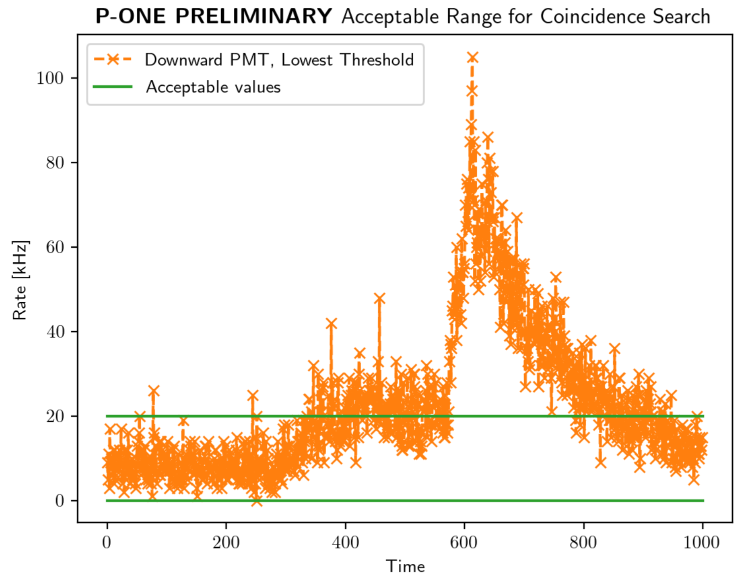

Figure 7: Example data showing a low noise time. Coincidences were searched for in times where the noise rate was less than 20kHz when binned by the millisecond, as shown by the green line. Results are **PRELIMINARY**

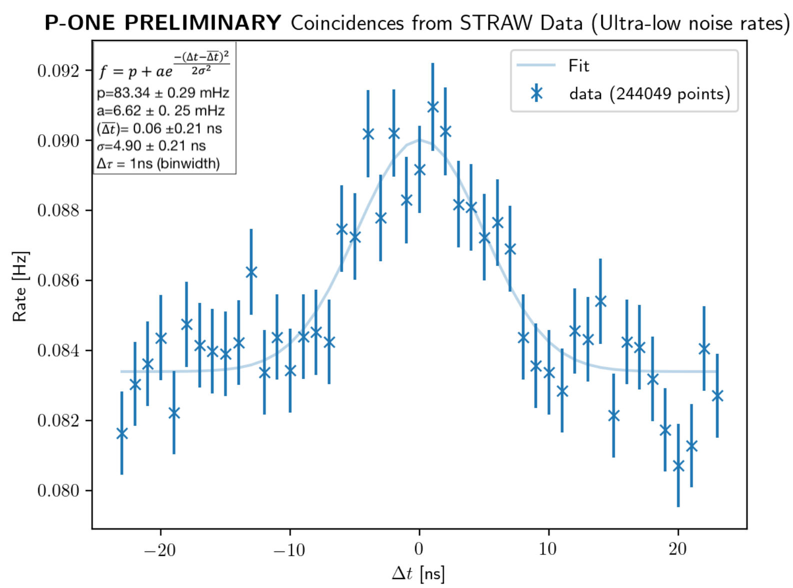

Figure 8: Detected hit time differences, Δt, between upward and downward facing PMTs on a single sDOM with Gaussian fit parameters listed. This distribution only emerges when we filter for the ultra low noise as seen in Figure 7. Results are **PRELIMINARY**

2.2 Simulation of STRAW detector

The activity of ^{40}K in the ocean water can be found from this distribution according to the equation:

$$B_q = \frac{1}{V_c}\frac{a\sigma\sqrt{2\pi}}{\Delta\tau} \tag{1}$$

where B_q is the activity of ^{40}K , a and σ are the amplitude and standard deviation of the Gaussian fit of the data, respectively, $\Delta\tau$ is the bin width of the distribution, and V_c is the effective detector volume for genuine coincidences. V_c can be found from simulations of the detector and represents the size the detector would have if every particle generated in a simulation of the detector resulted in a genuine coincidence. In other words,

$$V_c = \frac{n_d}{n_{gen}}V_{gen} \tag{2}$$

Where n_d is the number of detected coincidences, n_{gen} is the number of generated particles, and V_{gen} is the generated volume. GEANT4 was used to perform the detector simulation and find the effective volume.

Along with being able to calculate the effective detector volume, building an accurate simulation of our detector in its environment allows us to check our understanding of the detector and its systems and build a model of what is happening when we take data. Different components of noise can be added into the simulation and checked against the actual data to verify our understanding of the noise.

2.2.1 GEANT4 Simulation Details

For efficiency purposes, it was decided to only simulate the electrons emitted from a beta decay of ^{40}K instead of all the decay products. Electrons were generated with energies according to the decay energy of ^{40}K , normally distributed with a mean of 0.7 MeV, standard deviation of 0.4 MeV, minimum energy of 0.05 MeV and maximum energy of 1.31 MeV.[5] These electrons were generated at random locations in a sphere of water of radius 20m. This radius was chosen to maximize efficiency while detecting the most coincidences. In a simulation with a radius of 50m, 98.8% of genuine coincidences were within 20m of the centre of the sphere. When searching for only single hits the radius was increased to 50m and 100m due to the long absorption lengths of photons in water.

The absorption lengths for photons in water were also added into the simulation. Since there is not one length for all photon energies, values for the absorption length as a function of photon energy were added into the simulation according to Figure 9. As a first approximation, steps were used to simulate the absorption length function.

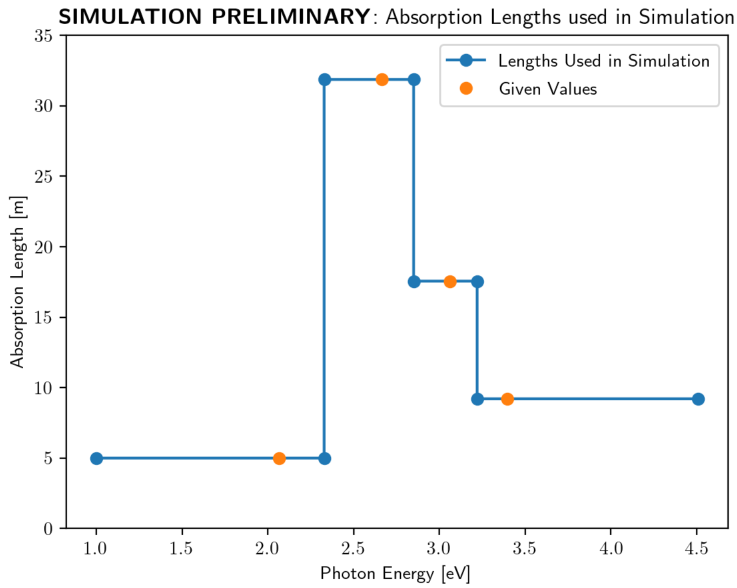

Figure 9: Plot of simulated absorption length as a function of photon energy, the blue curve represents the function input into the simulation with the orange dots representing the values found for the absorption length by other group members. Results are **PRELIMINARY**

2.2.2 Detector Definition

In order for our detector response to be as accurate as possible we tried to replicate the sDOM as best we could in our simulation. Two spherical sections of glass were placed inside larger hemispheres of glass to simulate the PMTs inside their glass housings. These hemispheres were placed on the two ends of a titanium cylinder with the same length as the sDOM. See Figure 10 for a comparison of the simulated sDOM to the actual sDOM.

In order to check how close the simulated sDOM was to the actual sDOM, an angular acceptance simulation was conducted. Photons were generated with isotropic momentum 25cm away from the sDOM with angles from 0 to 180 degrees in 10 degree increments. The number of detected photons at each angle was compared to the number of detected photons at 0 degrees and the results were plotted and compared to the angular acceptance of the actual sDOM [2]. See Figure 11. This simulated sDOM matched closely with the actual sDOM in angular acceptance and was used for all simulations.

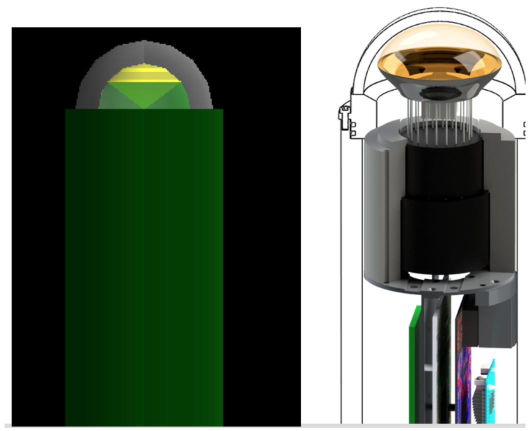

Figure 10: **PRELIMINARY** Comparison of simulated sDOM to actual sDOM. **Left**: The simualted sDOM. White represents glass, yellow represents the PMT and green represents Titanium. **Right**: Diagram of the actual sDOM. All lengths and sizes were matched as best as possible from schematic diagrams of both the sDOM itself and the PMT used in the sDOM. Right taken from [2]

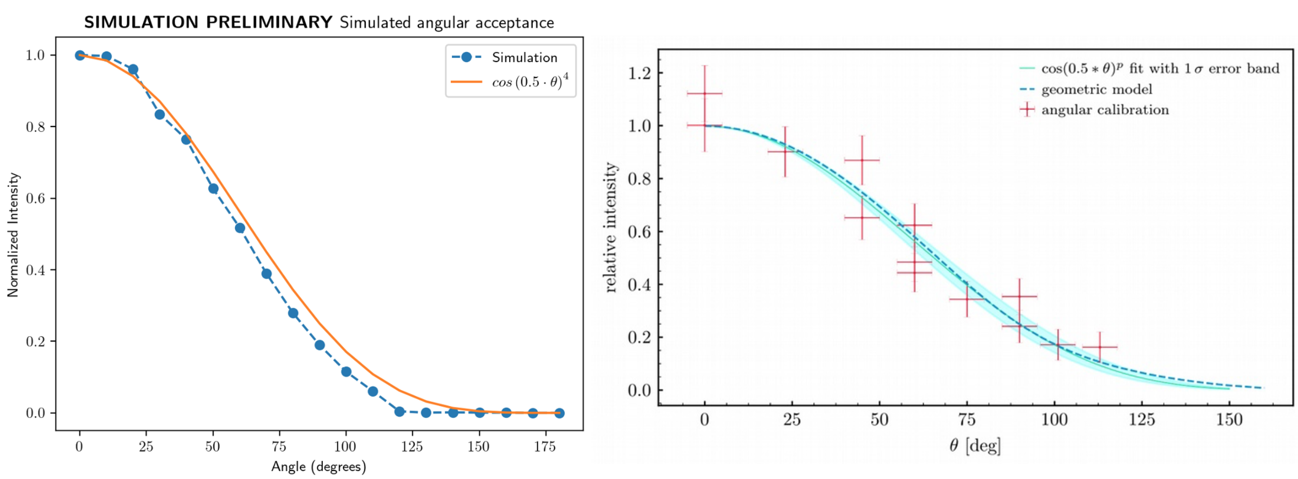

Figure 11: Plots of angular acceptance of simulated sDOM and actual sDOM. **Left**: Plot of simulated sDOM angular acceptance, the orange curve represents a fit of the actual sDOM acceptance. **Right**: Plot of the actual sDOM angular acceptance, taken from [2]. Results are **PRELIMINARY**

2.2.3 Quantum Efficiency

Every PMT has a certain energy range where it is best at detecting photons and even at this ideal energy range, every photon will not be detected. The percentage of photons which are detected at a certain energy for a PMT is known as its quantum efficiency (QE). The photons from the Cerenkov light of the decay electrons are spread out in energy and so the QE for the sDOM PMTs needed to be considered when modelling the sDOM response.

The QE for the sDOM PMTs had already been measured and published by KM3Net [6] and this data was used to model the QE of the sDOMs. The plot[7] of the QE can be seen in Figure 12. In the simulation the energy of each detected photon was recorded. After the simulation the energies were run through a script which weighted each detected photon according to the QE at that photon's energy.

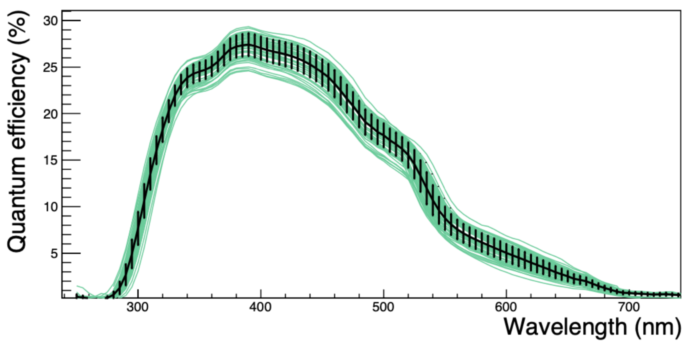

Figure 12: PMT quantum efficiency as a function of photon wavelength from [6]. This was used to weight each detected photon in simulation. Taken from [6]

2.2.4 Other Considerations

In order to further increase the accuracy of the simulation a few other sources of noise were added. These sources did not affect the rate of coincidences seen from ^{40}K but do contribute when trying to match the simulation with what is seen in the STRAW data.

^{40}K in glass. The glass hemispheres surrounding each PMT contain a small amount of ^{40}K (approximately 3 mBq for both hemispheres [8]). This rate was injected into the simulation similarly to the ^{40}K in the water. The ^{40}K was randomly distributed in the glass hemispheres with the same decay energies and with a Poisson distributed rate with a mean of 3 mBq for both hemispheres combined. The Cerenkov photons from the decay electrons were detected as an additional noise.

Dark Rate. Thermionic emissions in the PMT also contribute to a dark rate in the PMT. This dark rate has been measured at 2kHz at 20°C. This dark rate was also added to the data after simulation as a Poisson distributed noise with a mean of 2 detections per millisecond (2kHz).

Smearing. Even though the data from the STRAW detector reads out to the nanosecond, the electronics still smear that data reading and this needs to be considered in the simulation. For the PMT, the electron transit time spread (TTS) can be used as a value for the smearing. For the STRAW PMTs a TTS of 3.5 ns full width half maximum was found [2] and this was used to smear the simulated data.

Once these sources of noise had been considered and added into the simulation a plot was made to compare the results of the simulation to the actual STRAW data. This plot can be seen in Figure 13. Even though the largest simulation carried out simulated a sphere with a radius of 100m there is still some source of noise we are missing at these low noise times. Further thought needs to be put into finding what this source is.

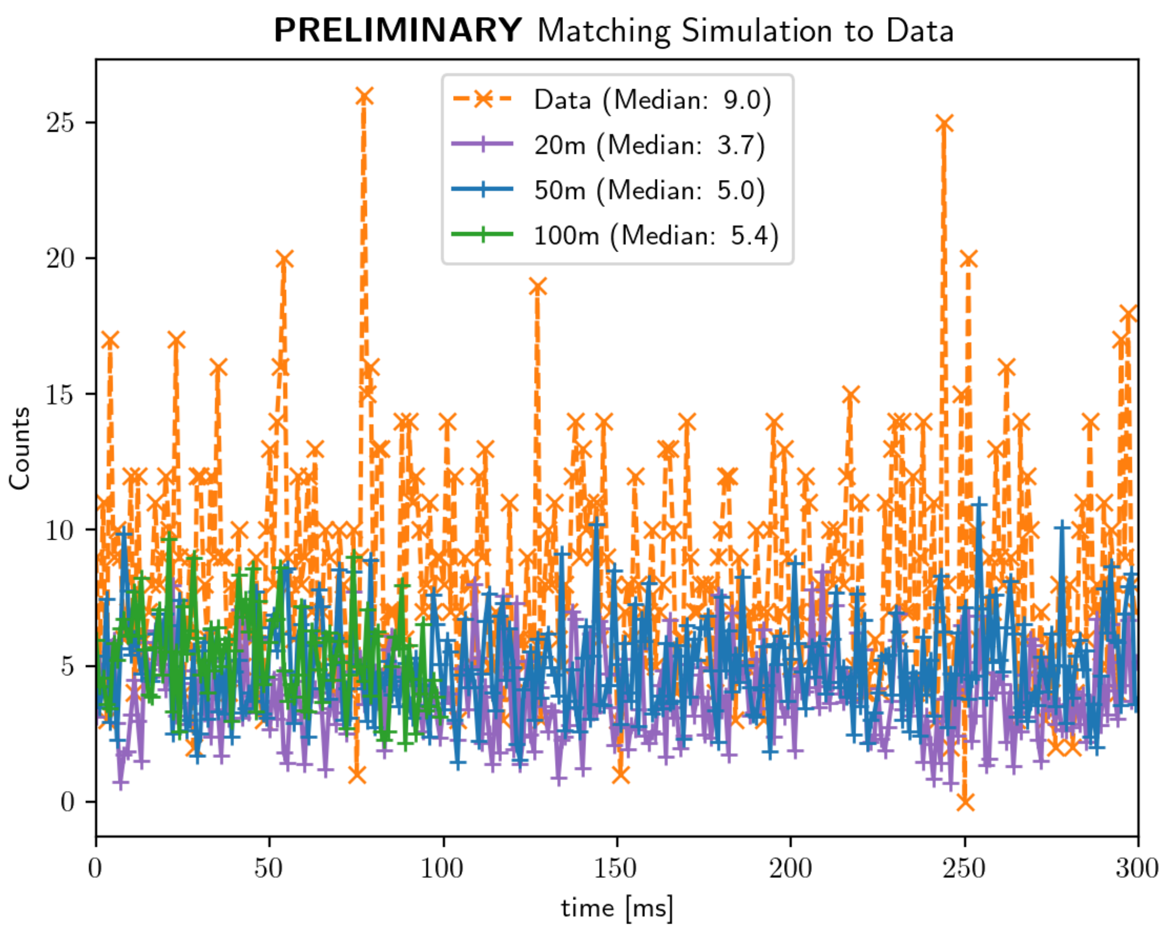

Figure 13: Simulated noise compared to straw data. The noise was simulated with multiple simulation volumes. The noise gets close to matching with the data with increasing radius but there is still some source of noise missing. Results are **PRELIMINARY**

2.2.5 Simulated Coincidences and Effective Volume

With all of the simulation details in place we can run the same search for coincidences as we did with the STRAW data and calculate the effective volume for simulation and the calculation of the Cascadia Basin salinity.

A plot of the simulated coincidences can be seen in figure 14. If the parameters of the Gaussian fit on this distribution of coincidences are compared with the parameters from the STRAW data fit, we see that the peak of the simulated coincidences is too narrow and there is some sort of smearing in the data we are not adding in properly. The smearing used comes from the electron transit time spread of the bare PMT so there may be extra smearing from the integrated PMT but this requires further investigation.

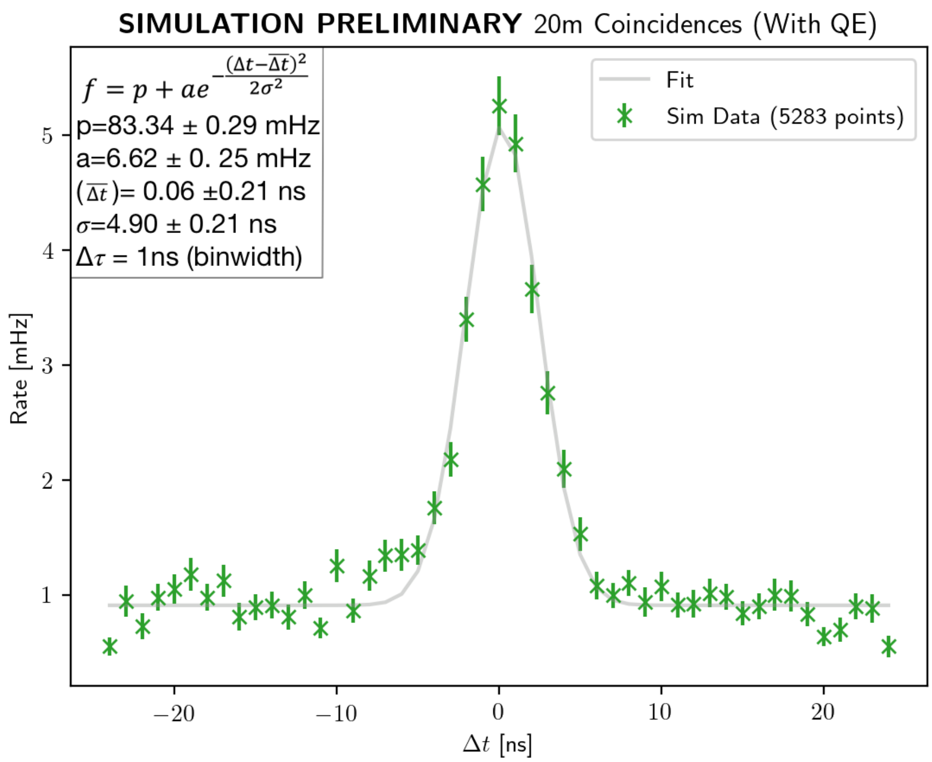

Figure 14: Detected hit time differences Δt, between upward and downward facing PMTs of a single simulated sDOM with Gaussian fit parameters listed. Results are **PRELIMINARY**

Using the simulated coincidences we can calculate the effective volume for simulation according to equation 2. With a generated volume from a sphere of radius 20m we calculate an effective volume of $6.47 \pm 0.12 \mathrm{cm}^3$. By recording the position of origin of each detected photon and scaling the number of generated particles, the effective volume as a function of radius can be determined and plotted. This plot is shown in Figure 15 and confirms that a sphere of radius 20m is sufficient for calculating the effective volume.

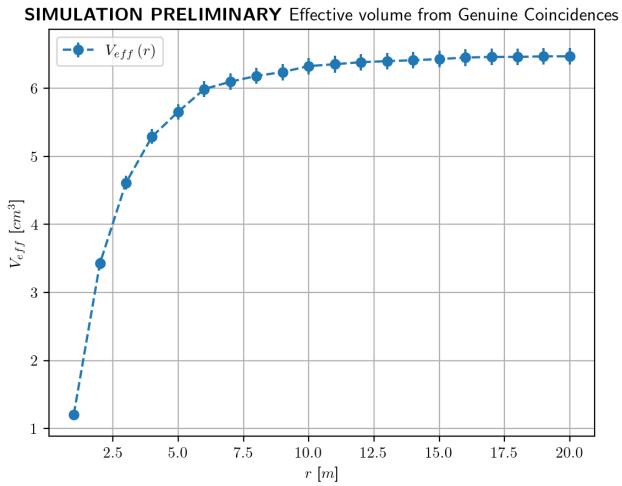

Figure 15: Plot of effective volume as a function of radius. The curve flattens as we approach the 20m radius suggesting that further increase in radius will not change the effective volume considerably. Results are **PRELIMINARY**

2.3 Salinity Calculation from ^{40}K coincidences

Using the fit parameters from the STRAW data along with the effective volume found from simulation, the ^{40}K decay rate can be found according to equation 1.[4] Plugging in all parameters, a ^{40}K decay rate of 12526 ± 752 ^{40}K decays per second per cubic metre. This number can be compared to the ocean salinity measured according to [9]

$$B_q = r_s \cdot r_K \cdot r_I \cdot \rho \frac{\ln 2}{\tau_{1/2}} \frac{N_A}{A} \tag{3}$$

Where r_s is the ocean salinity, $\tau_{1/2}$ is the half life of ^{40}K , A is the atomic weight of ^{40}K , 39.96 [4], N_A is Avogadro's Number, r_K is the potassium fraction of the salt in the ocean, 1.11%, r_I is the isotope fraction of ^{40}K , $1.17 \cdot 10^{-4}$, and ρ is the density of the seawater at the Cascadia Basin, 1.013 g/cm^3.

With a salinity value of 3.48% from Ocean Networks Canada [9] we find the true ^{40}K decay rate in the Cascadia Basin at 12 133 ^{40}K decays per second per cubic metre and our measurement of the ^{40}K decay rate with the STRAW detector is accurate error.

This measurement is significant as it is one of the first measurements made by the STRAW detector outside of its design of detecting and measuring POCAM flashes and shows we have an understanding of the ^{40}K noise in the Cascadia Basin. This measurement also allows us to use ^{40}K decay as a standard candle to measure our detector efficiency over time since the salinity of the Cascadia Basin will not change significantly over the lifetime of the detector.

3 Future Work

Although significant progress towards a noise model for P-ONE was made over the summer there are still some things that need to be addressed and further research needs to be done if a complete noise model is to be made. Other sources of noise including scintillation from the sDOM glass and bioluminescence noise should be analyzed and accounted for in the noise model and an ongoing analysis of the sDOM efficiency from the ^{40}K coincidences could also be set up.

3.1 Other Sources of Noise

The work done over this summer focused mainly on noise from ^{40}K since this noise is the most similar to the neutrino events we are trying to reconstruct. There are, however, other sources of noise that need to be looked into: mainly scintillation and bioluminescence.

3.1.1 Scintillation

Scintillation occurs when a high energy photon enters the glass hemisphere surrounding the PMT or the PMT itself. The photon interacts with the glass producing light that the PMT detects. High energy cosmic rays or other sources of high energy photons enter the detector at random times and cause scintillation noise in the data. This noise could be implemented into the current GEANT4 simulation of STRAW without too much difficulty as GEANT4 already has functionality for scintillation.

3.1.2 Bioluminescence

The ocean is full of microscopic life that emits light randomly or when disturbed. These bioluminescent organisms provide an additional source of noise which should be added to the model. A team within the P-ONE collaboration is already working on modelling the bioluminescence for P-ONE and their findings should be combined with this model to have a complete noise model for P-ONE.

3.2 Analysis of sDOM efficiency

Since we are able to accurately measure the salinity of the Cascadia Basin with the STRAW detector using coincident ^{40}K decays, a test of the sDOM efficiency over time could be implemented. Since the software to analyze STRAW data for coincidences already exists, running this test would only require taking more data at a later date and running the software over the new data. The new calculated salinity could be found and compared with the

ONC measurement to check if the detector efficiency has changed and if it is necessary to recalibrate the detector. Results from a long term study of detector efficiency could also be used to track sedimentation on the sDOMs over time.

4 Conclusion

Over the course of the summer progress was made towards a noise model for the P-ONE neutrino telescope using the STRAW detector with the main focus being on noise from Potassium-40.

A study of the noise from Potassium-40 (^{40}K) causing coincident hits on the detector was conducted and the salinity of the Cascaia Basin was found to be 12526 ± 752 ^{40}K decays per second per cubic metre which agreed with Ocean Netoworks Canada's measurement of the salinity within error. A simulation of STRAW was also created to model the noise from ^{40}K and to check our understanding of both the STRAW detector and ^{40}K noise. Other sources of noise can be added to this simulation to accurately model all sources of noise for the STRAW detector

5 Acknowledgements

I would like to thank all the members of the P-ONE collaboration for the opportunity to work on this project and for the feedback at our bi-weekly meetings. I would also like to thank the analysis group at the University of Alberta for their input and ideas for ways to increase the accuracy of my simulation. Finally I would like to thank my supervisor Matthias Danninger for this opportunity to take part in this research along with all of the input and help throughout the project, his positive attitude and encouragement made this research project extra enjoyable and I am very grateful he took me on to be his student.

References

[1] The P-ONE Collaboration, P-ONE.

[2] M. Boehmer et al., Journal of Instrumentation **14**, P02013 (2019), Publisher: IOP Publishing.

[3] S. Agostinelli et al., Nuclear Instruments and Methods in Physics Research Section A: Accelerators, Spectrometers, Detectors and Associated Equipment **506**, 250 (2003).

[4] A. Albert et al., The European Physical Journal C **78**, 669 (2018), arXiv: 1805.08675.

[5] G. Fiorentini, M. Lissia, and F. Mantovani, Phys. Rep. **453** (2007).

[6] ANTARES Collaboration et al., Journal of Instrumentation **13**, P05035 (2018), Publisher: IOP Publishing.

[7] A. Rohatgi, WebPlotDigitizer, 2020.

[8] (internal note).

[9] Ocean Networks Canada Data Archive.

Appendix: Example STRAW data

A sample of data from the STRAW detector. The first column represents the channel the hit occurred on, the second column the edge (0 rising, 1 falling) and the third column the detection time

1	0	81264.9
1	1	81298.5
1	0	90173.0
1	1	90206.4
2	0	43307.8
2	1	43339.1
2	0	43528.2
2	1	43562.6
2	0	55366.3
2	1	55399.4
2	0	73258.7
2	1	73289.9
5	0	14597.2
5	1	14635.2
5	0	26051.6
5	1	26087.0
9	1	4945.1
9	0	99914.9
0	0	200000.0
1	0	105105.3
1	1	105139.9
1	0	108241.6
1	1	108277.1
1	0	114799.6
1	1	114832.4
1	0	116739.0
1	1	116774.6
1	0	117630.5
1	1	117663.8